Development 134, 945-957 (2007) doi:10.1242/dev.02795

Fxna, a novel gene differentially expressed in the rat ovary at the time of folliculogenesis, is required for normal ovarian histogenesis

Cecilia Garcia-Rudaz[1,*], Felix Luna[1,*,†], Veronica Tapia[1,‡], Bredford Kerr[1], Lois Colgin[2], Francesco Galimi[3,4], Gregory A. Dissen[1], Neil D. Rawlings[5] and Sergio R. Ojeda[1,§]

In rodents, the formation of ovarian follicles occurs after birth. In recent years, several factors required for follicular assembly and the growth of the newly formed follicles have been identified. We now describe a novel gene, *Fxna*, identified by differential display in the neonatal rat ovary. *Fxna* encodes an mRNA of 5.4 kb, and a protein of 898 amino acids. Fxna is a transmembrane metallopeptidase from family M28, localized to the endoplasmic reticulum. In the ovary, Fxna mRNA is expressed in granulosa cells; its abundance is maximal 48 hours after birth, i.e. during the initiation of follicular assembly. Reducing Fxna mRNA levels via lentiviral-mediated delivery of short hairpin RNAs to neonatal ovaries resulted in substantial loss of primordial, primary and secondary follicles, and structural disorganization of the ovary, with many abnormal follicles containing more than one oocyte and clusters of somatic cells not associated with any oocytes. These abnormalities were not attributable to either increased apoptosis or decreased proliferation of granulosa cells. The results indicate that Fxna is required for the organization of somatic cells and oocytes into discrete follicular structures. As an endoplasmic reticulum-bound peptidase, Fxna may facilitate follicular organization by processing precursor proteins required for intraovarian cell-to-cell communication.

KEY WORDS: Ovarian development, Peptidases, Follicular assembly, Follicular growth, siRNAs

INTRODUCTION

In recent years, substantial progress has been made towards the identification of genes controlling the assembly and initial growth of ovarian follicles. Along the developmental pathway leading to the formation of ovarian follicles, three genes have been shown to play crucial roles in specifying the fate of germ cells: bone morphogenetic protein 4 (Bmp4), required for the generation of germ cells in the primitive epiblast (Lawson et al., 1999), stem cell factor (SCF) necessary for germ cell survival during migration towards the genital ridge (Godin et al., 1991), and wingless-related MMTV integration site 4 (Wnt4), a member of the Wnt family of locally acting cell signals, which is required for intragonadal survival of newly formed oocytes (Vainio et al., 1999). The formation of primordial follicles requires a transcription factor termed factor in the germline alpha (FIGα) (Liang et al., 1997). Subsequent differentiation and growth of primordial follicles is regulated by several factors produced locally by either granulosa cells or the oocyte itself. Granulosa cell factors that facilitate follicle growth include the kit ligand KL (Kitl) (Huang et al., 1993; Parrott and Skinner, 1999), basic fibroblast growth factor (bFGF; also known as Fgf2) (Nilsson et al., 2001), leukemia inhibitory factor (Lif) (Nilsson et al., 2002), the neurotrophins nerve growth factor (NGF), neurotrophin-4/5 (NT-4/5; also known as Ntf5), and brain-derived neurotrophic factor (Bdnf) (Dissen et al., 2001; Paredes et al., 2004; Spears et al., 2003), and others (Skinner, 2005). Oocyte factors implicated in the control of follicular growth include: growth differentiation factor 9 (Gdf9) (Dong et al., 1996), the homeobox gene *Nobox* (newborn ovary homeobox-encoding gene) (Rajkovic et al., 2004; Suzumori et al., 2002) and the TrkB receptors, which are high-affinity tyrosine kinase receptors for NT-4/5 and Bdnf (Paredes et al., 2004; Spears et al., 2003).

Identification of these key molecules has made it evident that follicular assembly, and the subsequent initiation of gonadotropin-independent follicular growth, require not only genes necessary for the specific development of germ and somatic cells, but also genes that promote and maintain the structural organization of the gland. We have now identified a gene that appears to be required for the structural organization of the rodent ovary. This gene, which we have termed Felix-ina (*Fxna*), encodes a novel member of the M28 family of metallopeptidases (Rawlings and Barrett, 1995). Our results suggest that Fxna plays a crucial role in processing proteins required for the organization of somatic cells and oocytes into follicular structures. A partial report of these findings has appeared in an abstract form (Garcia-Rudaz et al., 2004).

MATERIALS AND METHODS

Animals and tissues

Timed-pregnant Sprague-Dawley rats were purchased from B and K Universal (Fremont, CA). The ovaries were collected from fetuses at 21 days of gestation (F21), at different early postnatal (PN) ages (24, 48, 96 and 144 hours), PN-day 21, and from 60- to 90-day-old adult rats. In one study, other tissues were collected from PN-48-hour female rats for northern blot analysis. Upon collection, tissue samples were either frozen on dry ice for RNA extraction, or were fixed in either Bouin's fixative for paraffin embedding or in 4% paraformaldehyde-borate buffer, pH 9.5, for in situ hybridization. The rats were maintained and experimental procedures

[1]Division of Neuroscience and [2]Division of Animal Resources, Oregon National Primate Research Center/Oregon Health and Science University, 505 N.W. 185th Avenue, Beaverton, OR, USA. [3]University of Sassari Medical School/INBB, Italy. [4]The Salk Institute, San Diego, CA, USA. [5]The Sanger Institute, Wellcome Trust Genome Campus, Hinxton, Cambridge CB10 1SA, UK.

*These authors contributed equally to this work
†Present address: Facultad de Ciencias Quimicas, Benemerita Universidad Autonoma de Puebla, Puebla, Mexico
‡Present address: Laboratorio de Bioquimica, Departmento de Ob/Gyn, Hospital Clinico, Universidad de Chile, Santiago, Chile
§Author for correspondence (e-mail: ojedas@ohsu.edu)

Accepted 18 December 2006

conducted in accordance with the principles outlined in the National Research Council's Guide for the Care and Use of Laboratory Animals under a protocol approved by the ONPRC Animal Care and Use Committee.

RNA isolation

Total RNA was extracted using the acid-phenol method (Chomczynski and Sacchi, 1987) for use in the gene differential display and RNase-protection assays, or using TRI Reagent (Molecular Research Center, Cincinnati, OH) (Mungenast and Ojeda, 2005) for use in all other procedures.

Gene differential display

For identification of genes differentially expressed at the time of follicular assembly we used a Differential Display Kit (GeneHunter, Nashville, TN), as described (Paredes et al., 2005). The sequences obtained were compared with gene sequences available in GenBank using the Basic Local Alignment Search Tool (BLAST) algorithm applied to searches of the non-redundant (nr) and Expressed Sequence Tag (EST) NCBI databases.

RNase-protection assay and cRNA probes

RNase-protection assays (Gilman, 1993) were carried out as described previously (Dissen et al., 1995; Ma et al., 1996) using 10 μg total RNA per tube. Cyclophilin mRNA, which is constitutively expressed in the ovary, was used to normalize *Fxna* mRNA values. The antisense RNA probes used to detect *Fxna* transcripts were transcribed from two DNA templates derived from the coding region of *Fxna* mRNA (probe A, 292 nt, complementary to nt 4846-5138 in NM_184050; probe B, 488 nt, complementary to nt 1591-2079). The cyclophilin probe (158 nt) is complementary to nt 265-422 of rat cyclophilin mRNA (M19533).

Northern blots

Polyadenylated RNA was isolated from total RNA extracted from various tissues of 2-day-old female rats using the MicroPolyA-Purist Kit (Ambion, Austin, TX). Northern blotting was performed as described (Lara et al., 1990; Trzeciak et al., 1987), using 5 μg of mRNA per lane.

In situ hybridization

The in situ hybridization procedure employed (Simmons et al., 1989) was carried out as previously reported (Dissen et al., 1991; Dissen et al., 1995) using 14 μm cryostat sections and *Fxna* cRNA probe A labeled with ^{35}S-UTP. Control sections were hybridized to a sense Fxna probe transcribed from the same cDNA template but in the opposite direction.

PCR cloning

To sequence *Fxna* mRNA, we PCR-amplified overlapping portions of the mRNA from ovarian RNA beginning from the 3′ end using, as a starting point, the sequence of the C5-530a2 cDNA identified by gene differential display. The primers used are listed in Table 1.

The coding region of *Fxna* mRNA was cloned using the FailSafe PCR System Kit (Epicentre Biotechnologies, Madison, WI) and primers (forward, 5′-TATAGATCTTGGAGTGGAGCTCGGAAGT-3′; reverse, 5′-TAT-AGATCTTTAAAACACAAAGAGACTATAGGTGG-3′), containing a *Bgl*II site at their 5′ ends (underlined). The PCR product was cloned into the pGEM-T vector (Promega, Madison, WI) and sequenced from both ends, before cloning into the *Bgl*II site of the expression vector pCMV-Tag1 (Stratagene, San Diego, CA).

A tagged Fxna construct was generated by PCR-amplifying the *Fxna* coding region from ovarian RNA with a sense primer (5′-GGATCCGCTGCCGCCATGGAGTGG-3′) and an antisense primer (5′-GATATCATATTA*CTTGTCGTCATCGTCTTTGTAGTC*AAACACAAAGA-GACTATA-3′) that contains a FLAG epitope-coding sequence (in italics); *Bam*H1 and *Eco*RV sequences added to the sense and antisense primers, respectively, are underlined. The resulting construct was ligated into pcDNA-Zeo (Invitrogen).

siRNA synthesis and transfection

Five siRNAs were synthesized by in vitro transcription with T7 RNA polymerase using the Silencer siRNA Construction Kit (Ambion). The siRNAs were named according to their position in the coding region of *Fxna* mRNA (i.e. starting at 436, 571, 724, 975 and 1239 nt, where ATG=+1).

siRNA 436: sense, 5′-AACAGCCTCCACAGAATCTCA-3′; antisense, 5′-AATGAGATTCTGTGGAGGCTG-3′;
siRNA 571: sense, 5′-AAGTACGCTGTCCTGGCTAAC-3′; antisense, 5′-AAGTTAGCCAGGACAGCGTAC-3′;
siRNA 724: sense 5′-AATGGTGCAGAGGAAAATGTC-3′; antisense, 5′-AAGACATTTTCCTCTGCACCA-3′;
siRNA 975: sense 5′-AATCTACAGGGATTTTGGGAA-3′; antisense, 5′-AATTCCCAAAATCCCTGTAGA-3′; and
siRNA 1239: sense, 5′-AATAAACTACATGGTGGTAAT-3′; antisense, 5′-AAATTACCACCATGTAGTTTA-3′.

The effectiveness of these siRNAs was tested using rat kidney embryonic cells (RK3E) and human 293T cells. The cells were maintained in DMEM (Sigma, St Louis, MO) supplemented with 10% heat-inactivated FBS (HiClone, Logan, UT), and containing penicillin G (100 U/ml; Sigma) and streptomycin sulfate (100 μg/ml; Sigma). The medium for 293T cells also contained 50 μg/ml gentamycin. Cells were cultured at 37°C under a 5%-CO_2 95%-air atmosphere. Cells were seeded into 6-well plates (3×10^5 cells per well) 24 hours prior to transfection, in antibiotic-free DMEM medium. Each siRNA was transfected (at a 10 nM concentration) using the Gene

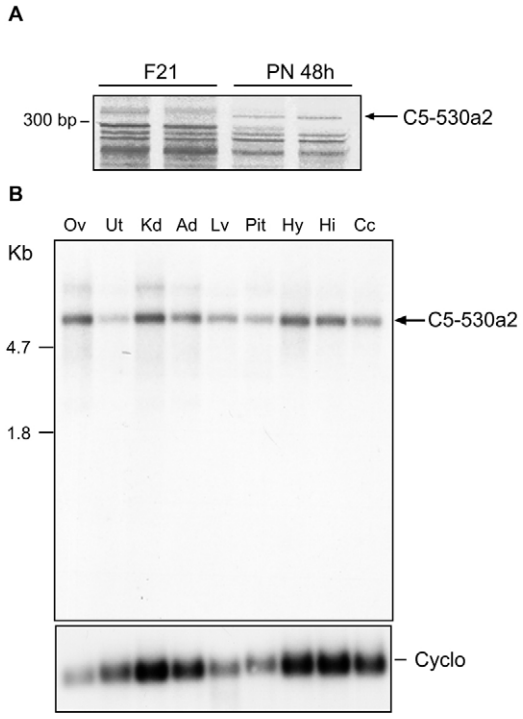

Fig. 1. A novel mRNA differentially expressed in the developing ovary of the rat is also expressed in several other tissues. (**A**) Autoradiograph of a sequencing gel showing that the signal intensity of a PCR product (C5-530a2, arrow) derived from the gene differential display amplification of total perinatal rat ovarian RNA is greater in samples from PN-48-hour than F21 ovaries. Each PCR reaction was electrophoresed in duplicate. (**B**) Northern blot analysis of polyA$^+$ RNA extracted from different tissues of 2-day-old female rats identifies a ubiquitous 5.4 kb mRNA species (arrow) and a longer, much less abundant transcript in ovary, kidney and adrenal gland. The cRNA probe used was transcribed from a C5-530a2 cDNA template. Each lane contains 5 μg of polyA$^+$ RNA. Cyclophilin mRNA (cyclo) detected subsequently on the same blot was used as a control for procedural variability. Migration of the 4.7 and 1.8 kb ribosomal RNA species detected by ethidium bromide staining is indicated on the left side of the blot. Note that cyclophilin mRNA expression is not constant across tissues. Ov, 2-day-old rat ovary; Ut, uterus; Kd, kidney; Ad, adrenal gland; Lv, liver; Pit, pituitary gland; Hy, hypothalamus; Hi, hippocampus; Cc, cerebral cortex.

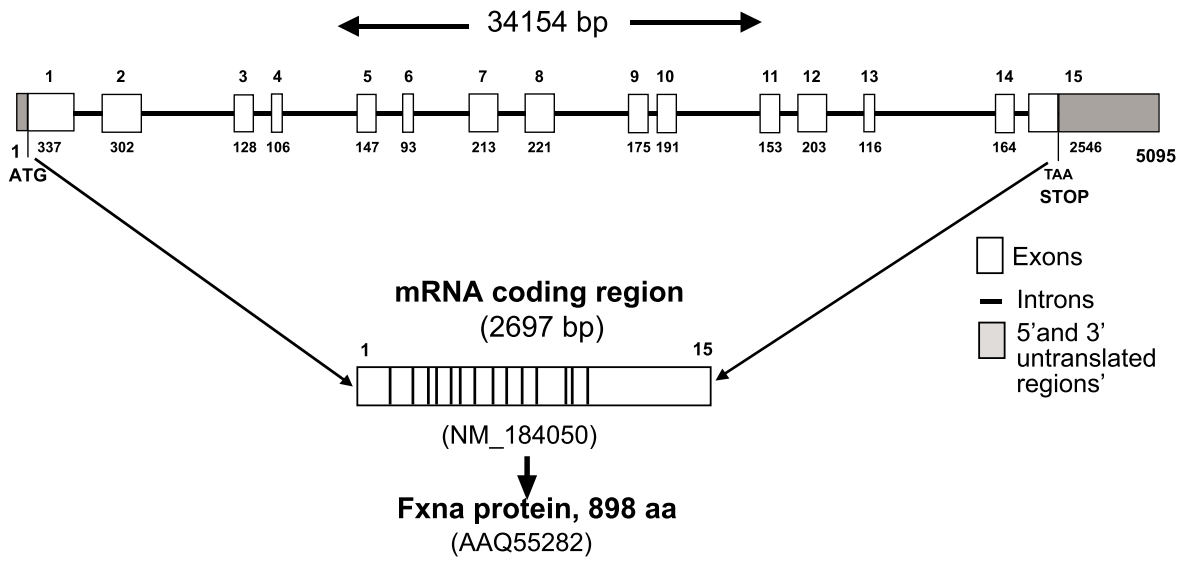

Fig. 2. Genomic structure of the C5-530a2 (*Fxna*) gene. Boxes represent exons, and the horizontal line connecting them represents introns. Gray boxes denote 5′- and 3′-untranslated regions. Exon number is given above each box; numbers beneath indicate the size (bp) of each exon.

Eraser Reagent (Stratagene). Cells were harvested 48 hours post-transfection, and total RNA extracted for PCR amplification. The sense primer used (5′-CCATCGGCCCCAGGACTA-3′) corresponds to nt 361-378 of rat *Fxna* mRNA (NM_184050), and the antisense primer (5′-AACACGAGAAGGGTACGCAATGAC-3′) is complementary to nt 1224-1247. As an internal control, we amplified a fragment from rat cyclophilin mRNA using a forward primer (5′-ACGCCGCTGTCTCTTTTC-3′) corresponding to nt 344-364 of rat cyclophilin mRNA (NM_19533), and a reverse primer (5′-CTTGCCACCAGTGCCATTAT-3′) complementary to nt 545-565. PCR amplification was performed using HotStart Taq polymerase (Qiagen, Valencia, CA). Equal volumes were electrophoresed on 2% agarose gels stained with ethidium bromide. Gel images were quantitated using Quantity One software (Bio-Rad Laboratories, Hercules, CA). The optical densities of *Fxna* mRNA were normalized to cyclophilin mRNA.

siRNA specificity

To assess the specificity of LV-sh436 we transfected 293T cells with an expression vector (pCMV-Tag1, Stratagene) encoding either an intact *Fxna* mRNA or *Fxna* mRNA carrying silent point mutations of the siRNA target region. The third base of each of two codons in this region was mutated (5′-AACAGCCTCCACAGAATaTCt), using the QuickChange XL Site-Directed Mutagenesis Kit (Stratagene). The cells (3×10^5 cells per well in 6-well plates) were transfected with either 70 ng pCMV-Fxna or pCMV-Fxna-Mutated using Lipofectamine 2000 (Invitrogen). Four hours after transfection, the cells were infected with LV-sh436 at a 10:1 virus:cell ratio, and the cells harvested 3 days after infection. *Fxna* mRNA was measured as outlined above, but cyclophilin mRNA was amplified with a set of primers targeting human cyclophilin (M80524). The sense primer (5′-GGGAAGTCCATCTACGGA-3′) corresponds to nt 432-450 of human cyclophilin mRNA, and the antisense primer (5′-ACATGCTTGCCATCCAAC-3′) is complementary to nt 571-599.

Design and cloning of shRNA-producing cassettes

Delivery of siRNAs via lentiviruses was carried out as described (Tiscornia et al., 2003). A cassette derived from the vector pSilencer 1.0-U6 (Ambion) was cloned into the 3′ long terminal repeat (3′-LTR; *Bbs*I site) of a lentiviral vector modified from that described by others (Follenzi et al., 2000). In this cassette, transcription of siRNAs is directed by the mouse RNA Polymerase III U6 promoter. In our plasmid, termed LV-EGFP, the original PGK promoter driving expression of an enhanced green fluorescent protein

Table 1. Primer sets used to amplify and sequence *Fxna* mRNA

Sense (5′ to 3′)	Location*	Antisense (5′ to 3′)	Location*
GGTGGGGCGGTTGG	–32 to –19	ACTAATGTCGTGGTGAAGCTGGAG	549-572
ATGGAGTGGAGCTCGGAG	18-36	ACTAATGTCGTGGTGAAGCTGGAG	549-572
ATGGAGTGGAGCTCGGAGT	18-37	TTCCACCTATAGTCTCTTTGTGTTT	2685-2711
AGCAAGCCATGGTTTTATTACTCA	767-790	ACTTTCATTAGCTGGTTCACC	1367-1388
CATTCATGAGTGCTGTCTGG	1647-1667	CAGTCCAAAGCCGAAGAGA	2036-2054
GCTCTTTACTTATTGGGGATGTTC	1743-1766	ATTGGTCATTTCCCTCGGA	2662-2679
GCTCTTTACTTATTGGGGATGTTC	1743-1766	TGTTTCATTTGTGCAAGCA	3356-3374
TCCCCAAGAAATCCTGCTC	2301-2319	TGAGGAGGAAGAGGAGGAGCG	3421-3441
AATTAACCCTCACTAAAGGG	T7 primer	GTTTCATTTGTGCAAGCA	3356-3374
″	T7 primer	TGAGGAGGAAGAGGAGGAGCG	3421-3441
″	T7 primer	GCAGAAGGGCAGCAGGAGAC	3672-3691
″	T7 primer	ATGTAGGGCTGCAGCTGGAG	4109-4118
″	T7 primer	TTGAGCCTTTATACTGCCTTTTC	4487-4509
″	T7 primer	TTTTGAAGATTACCTGACCAC	4713-4733
″	T7 primer	TACAGCATTTCCAGTTTAGCAGC	4873-4895
″	T7 primer	CTAAATGTCTAAGATCCCCCACC	4901-4923

*Numbers refer to position (nt) in *Fxna* mRNA relative to the ATG codon at +1.

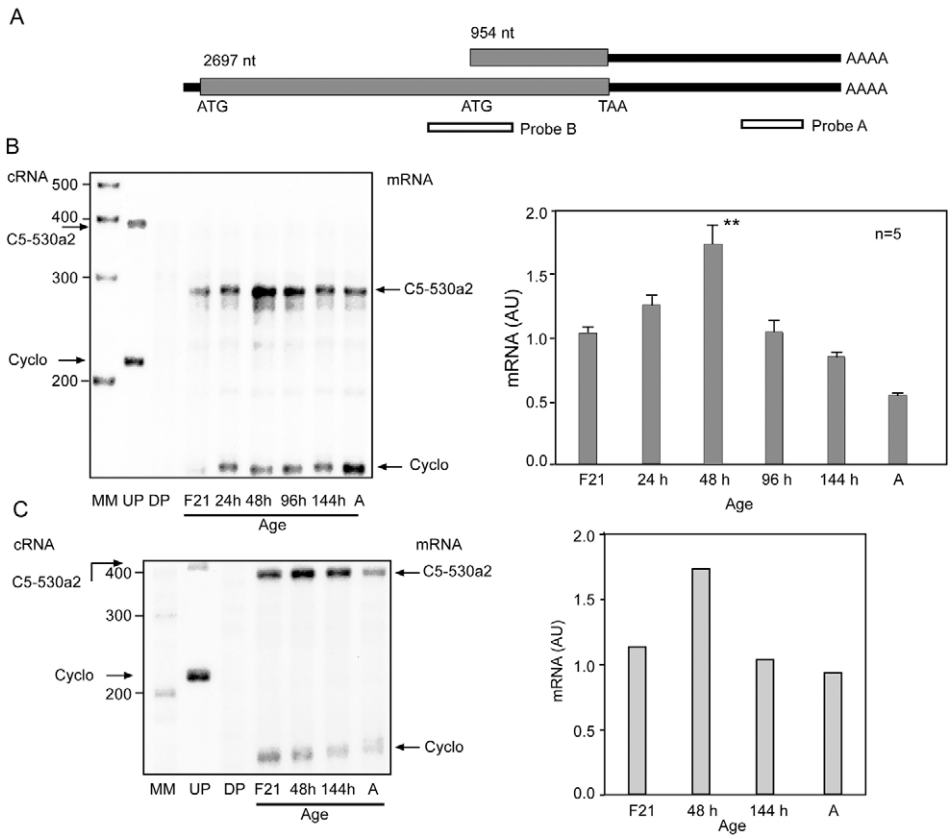

Fig. 3. Changes in C5-530a2 mRNA expression during early postnatal development of the rat ovary, as assessed by an RNase-protection assay. (**A**) Above: the hypothetical gene (BC031519) predicted to encode a 317 amino acid protein; beneath: C5-530a2 (NM_184050) that was demonstrated experimentally to have a longer open reading frame. The predicted coding regions are depicted in gray and the untranslated regions in black. The approximate locations of the two probes used for RNase-protection assay are shown as white rectangles. The two putative ATG sites are indicated. (**B**) Left panel shows a representative autoradiogram depicting the increase in C5-530a2 mRNA abundance (detected by RNase-protection assay using probe A) between F21 and PN 48 hours, and the decrease towards adult values seen thereafter. Probe A consists of 289 nt transcribed from a C5-530a2 cDNA template plus 88 nt derived from transcribed vector sequences. The cyclophilin probe (Cyclo) is 211 nt in length, of which 158 nt correspond to transcribed vector sequences. The mRNA species protected by probe A, and the cyclophilin cRNA probe, are arrowed. MM, molecular weight markers (^{32}P-labeled RNA ladder); UP, undigested probe; DP, digested probe; A, adult ovaries. Right panel is a densitometric analysis of the changes in C5-530a2 mRNA levels detected by RNase-protection assay. RNA abundance is expressed as arbitrary units (AU) calculated using the individual C5-320a2/cyclophilin mRNA ratios from each sample. **, P<0.02, 48 hour group versus all other groups. Bars are mean values for each group and vertical lines represent s.e.m. (**C**) The same RNase-protection assay analysis as in B, but using probe B and samples pooled from selected developmental ages. Probe B consists of 492 nt, of which 406 correspond to transcribed vector sequences.

(EGFP) (Follenzi et al., 2000) was replaced by a cytomegalovirus (CMV) promoter. The DNA sequence encoding the most potent siRNA (siRNA 436) was cloned into the *Apa*I-*Eco*RI sites of the multiple cloning site of the U6 cassette (see Fig. S1 in the supplementary material). We refer to this construct as LV-sh436. A DNA fragment encoding siRNA 436 with nucleotide mismatches (LV-sh436 mism, 5′-CAGGCTCGACAGTATC-TGA*TTCAAGAGA*TCAGATACTGTCGAGCCTG*TTTTTT*-3′; the hairpin loop and the polyT sequences are in italics; mismatches are underlined) was similarly cloned.

The lentiviral gene delivery system

This system, which represents a prototype of third-generation, safe, replication-defective lentiviral vectors (Dull et al., 1998; Follenzi et al., 2000), consists of two packaging plasmids (pMDLgpRRE, pRSV-Rev), an envelope plasmid (pMD.G) and a lentiviral vector plasmid (pLV, the ‘delivery vector’) that encodes an EGFP marker. The 3′-LTR is self-inactivating. Recombinant lentiviruses were produced by co-transfecting the four plasmids into 293T cells using the calcium phosphate method (Dull et al., 1998). The medium containing infectious viral particles was collected 24 and 48 hours after transfection and filtered through a 0.22 μm membrane (Steriflip; Millipore, Bedford, MA). Lentiviruses were concentrated by ultracentrifugation (2 hours, 53,000×***g***) and purified through 20% sucrose (2 hours, 45,000×***g***) (Tiscornia et al., 2003). Lentivirus titer was determined by flow cytometry (FACScalibur; BD Biosciences, San Jose, CA) using serial dilutions of the virus, and EGFP as the marker. The titer is expressed as transducing units (TU) per ml.

Interferon-like responses

To rule out non-specific mRNA degradation resulting from activation of the interferon system, semi-quantitative PCR was used to measure the mRNA content of 2′-5′ oligoadenylate synthase (*Oas1*), a major interferon target gene (Bridge et al., 2003), in untreated cultured ovaries and ovaries treated with LV-sh436, LV-sh436 mism or LV-EGFP. The primers used to detect *Oas1* were: sense, 5′-TACAATCCTGATCCC-AAGA-3′ corresponding to nt 538-559 of rat *Oas1* mRNA (NM_138913); and antisense, 5′-GAGCTCCGTGAAGCAGGTAGA-3′ complementary to nt 613-633.

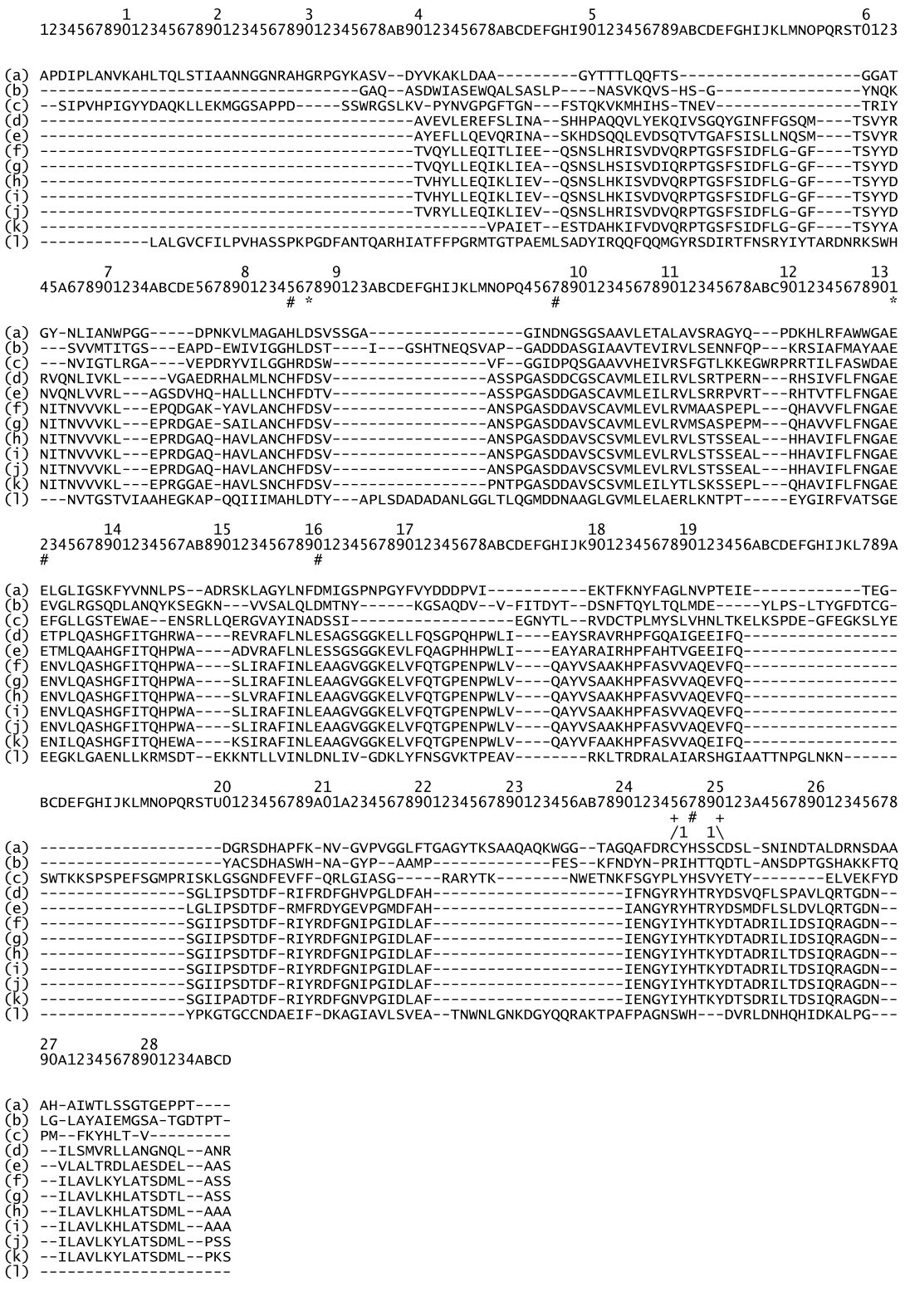

Fig. 4. Alignment of selected sequences from peptidase family M28. Sequences have been selected from an alignment of all known peptidase members of family M28. Sequences are numbered according to the type example for the family, aminopeptidase S (*Streptomyces griseus*). Active site residues are indicated by asterisks, and metal ligands by hash (#) symbols. The cysteines involved in the known disulfide bridge in aminopeptidase S are indicated (+). Cysteines taking part in the same disulfide bridge are denoted as /1 and 1\. Key to sequences: (a) aminopeptidase S (*Streptomyces griseus*); (b) aminopeptidase Ap1 (*Vibrio proteolyticus*); (c) glutamate carboxypeptidase II (*Homo sapiens*); (d) agCP10156 protein (*Anopheles gambiae*); (e) agCG47216 protein (*Anopheles gambiae*); (f) Fxna peptidase (*Rattus norvegicus*); (g) Fxna peptidase (*Mus musculus*); (h) Fxna peptidase (*Pan troglodytes*); (i) Fxna peptidase (*Homo sapiens*); (j) Fxna peptidase (*Canis familiaris*); (k) Fxna peptidase (*Gallus gallus*); (l) IAP aminopeptidase (*Escherichia coli*).

Fig. 5. Fxna functional domains. The deduced amino acid sequence is shown in capital letters and the nucleotide sequence in lower case letters. The peptidase unit is underlined; the catalytic residues (Asp 201, Glu 245) are circled, and the metal-binding amino acids (His 199, Asp 211, Glu 246, Glu 272 and His 348) within squares. Heavy underlining identifies the polyadenylation signal.

Organ culture

The ovaries from newborn rats (on day of birth), were cultured as described (George and Ojeda, 1987). One ovary from each animal was treated for 4 days with LV-EGFP and the contralateral ovary with LV-sh436, each at 4×10^6 TU per well. Some ovaries (two pools containing three glands per pool) were treated with LV-sh436 mism.

Proliferation and apoptosis

To assess proliferation, newborn rat ovaries were cultured as described above, and the culture medium supplemented with 100 μM bromodeoxyuridine (BrdU; Roche Diagnostics, Indianapolis, IN) 24 hours before termination of the culture. Thereafter, the ovaries were fixed in Kahle's fixative (Hirshfield and DeSanti, 1995), embedded in paraffin and sectioned at 6 μm. BrdU immunohistochemistry was performed using a monoclonal antibody (Mab-2531, 1:1000; Sigma) and the reaction was developed with DAB-nickel chloride (Dees et al., 1995). Ovary sections were imaged on a Marianas Imaging Workstation using Slidebook (Intelligent Imaging, Denver, CO), and a 10× NA 0.5 objective. BrdU-positive cells were counted using Metamorph (Universal Imaging, West Chester, PA) in 30 identical rectangles (70×52 pixels) corresponding to an area of 1456 μm^2, each uniformly distributed in a random fashion over four sections from each group.

Apoptotic ovarian cells were detected in 14 μm cryostat sections using the TUNEL assay according to the manufacturer's specifications (Roche Diagnostics).

Follicular development

Cultured ovaries were fixed in Kahle's fixative, embedded in paraffin, serially sectioned at 6 μm, and stained with Weigert's iron Hematoxylin and counterstained with picric acid-Methyl Blue (Dissen et al., 2001). Every third section was imaged on a Zeiss Axioplan (Carl Zeiss, Jenna, Germany), using a CoolSnap camera (Roper Scientific, Stillwater, MN). Follicles were counted using the manual count feature of MetaMorph (Universal Imaging, West Chester, PA) as reported (Dissen et al., 2001; Paredes et al., 2004).

Immunohistofluorescence-confocal microscopy

Ovarian cells infected by the lentivirus were visualized by immunofluorescence in 14 μm frozen sections using an anti-EGFP polyclonal antibody (Molecular Probes, Eugene, OR; 1:800, overnight incubation at 4°C). Immunoreactivity was developed using an Alexa 488-conjugated donkey anti-rabbit gamma globulin antibody (Molecular Probes; 1:200). Control sections were incubated without primary antibody. Images were acquired as previously reported (Dissen et al., 2001). Cell nuclei were stained with Hoescht 33258 (Invitrogen; 0.1 μg/ml KPBS for 1 minute after completion of the immunohistochemical reactions).

To determine the intracellular localization of Fxna, COS-7 cells (1.5×10^5 cells per well in 6 well plates, i.e. 15,000 cells/cm^2) were transfected with either 650 ng per well of Fxna-Flag-pcDNA or the empty vector (pcDNA3.1 Zeo) using Lipofectamine 2000. Twenty-four hours later the cells were fixed in acetone (1 minute at –20°C). Fxna-Flag was detected with an anti-Flag monoclonal antibody (M2, Sigma) at 1:1000 dilution, and the reaction was developed using an Alexa 488-conjugated donkey anti-mouse gamma globulin antibody (1:500). To visualize the endoplasmic reticulum, we used a rabbit polyclonal antibody (sc-20132, Santa Cruz; 1:250) against oxidoreductase-protein disulfide isomerase (PDI), an endoplasmic reticulum-specific protein. The PDI reaction was developed using Alexa 594-conjugated donkey anti-rabbit gamma globulin antibody (1:500). Cell nuclei were stained with Hoescht.

Statistical analysis

Comparisons between two groups were performed using either the unpaired (cell transfection studies) or paired (organ culture, morphometric studies) Student's *t*-test. Sequence comparisons were performed using BlastP (Altschul et al., 1990) against the non-redundant protein sequence database at NCBI (Benson et al., 2006), and using FastA (Lipman and Pearson, 1985) against the peptidase sequence collection compiled by the MEROPS database team (Rawlings et al., 2006).

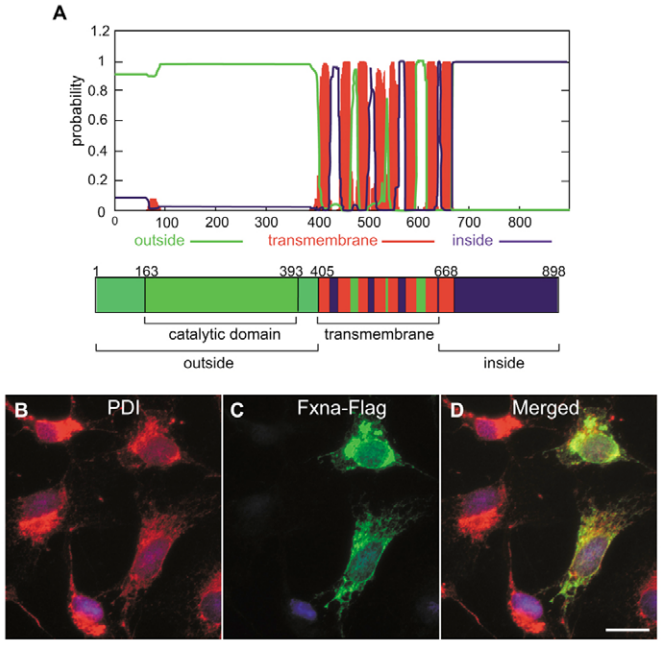

Fig. 6. The cellular localization of Fxna. (**A**) Predicted cellular localization domains of Fxna. The graph depicts the probability of different regions of the Fxna protein being located on the outer or inner side of a cellular membrane, or embedded within the membrane. Red, membrane-associated domains; green line, outer side of membrane; blue line, inner side of membrane. The catalytic domain is located on the outer side of a cellular membrane between amino acid residues 163-393. (**B-D**) Double immunohistofluorescence images showing the colocalization of Fxna-Flag (green) with PDI, an ER-specific marker (red). COS-7 cells were transfected with Fxna-Flag 24 hours prior to staining with a monoclonal antibody against Flag and a polyclonal antibody against PDI. Note that non-transfected cells are only positive for PDI. Cell nuclei are stained with Hoescht 33258 (blue). Scale bar: 20 μm.

RESULTS

A novel mRNA is differentially expressed in the developing rat ovary

Because folliculogenesis in the rat is initiated 48 hours after birth (Malamed et al., 1992; Rajah et al., 1992), we compared the expression profiles of RNA extracted from pools of F21 ovaries with those derived from ovaries dissected at PN 48 hours, using the technique of gene differential display (Martin and Pardee, 1999). An α-^{33}P-ATP-labeled band (C5-530a2) of approximately 300 bp (arrow in Fig. 1A) showing increased intensity at PN 48 hours was selected for further analysis. The PCR product showed strong similarity to a mouse hypothetical gene (BC031519) located on chromosome 19, predicted to encode a 3.3 kb mRNA species and a protein of 317 amino acids.

C5-530a2 mRNA is larger than the predicted mRNA and is expressed in several tissues of 2-day-old rats

The size of the predicted C5-530a2 mRNA was estimated by northern blot hybridization using a cRNA probe transcribed from C5-530a2 cDNA. The mRNA is widely expressed in rat tissues (Fig. 1B), with the greatest abundance seen in ovary, kidney and two areas of the brain (hypothalamus and hippocampus). Contrary to the predicted mRNA size of 3.3 kb, the northern blot showed the

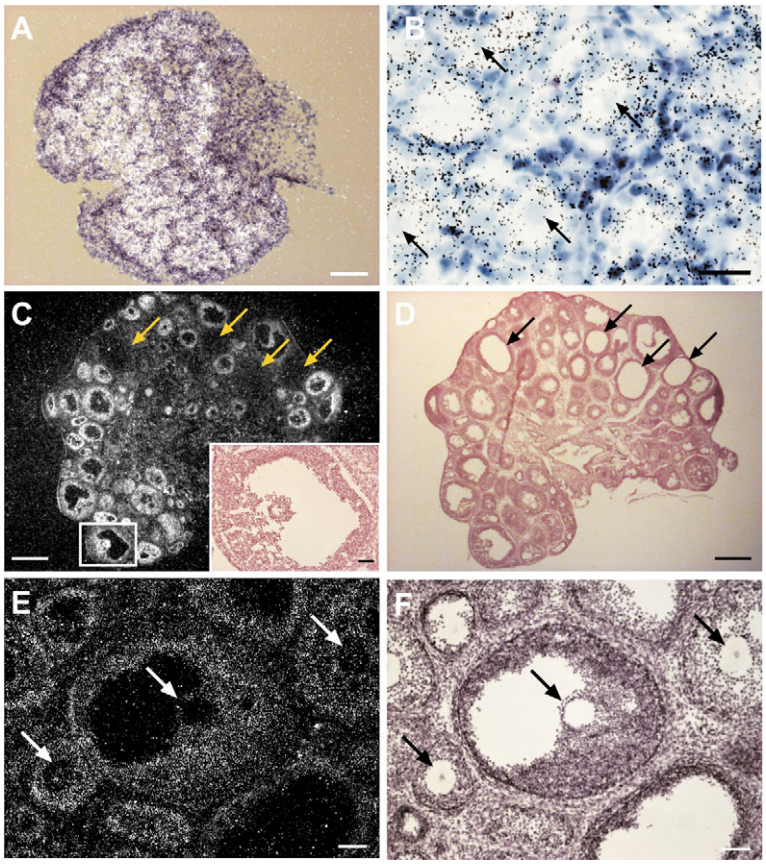

Fig. 7. *Fxna* mRNA is expressed in granulosa cells of the developing rat ovary. The mRNA was detected by in situ hybridization using ^{35}S-UTP-labeled Fxna cRNA probe B. (**A**) Low magnification dark-field image of a PN-48-hour ovary. Cell nuclei were stained with thionin (blue-purple); the hybridization signal in newly formed follicles is seen as white grains. (**B**) Higher magnification, bright-field image showing the presence of *Fxna* mRNA (black grains) in granulosa cells, but not oocytes (arrows) of a PN-48-hour ovary. (**C**) Low magnification, dark-field image of a 21-day-old ovary showing the presence of *Fxna* mRNA in granulosa cells of both preantral and antral follicles. Arrows point to atretic follicles devoid of hybridization signal. The inset is a higher magnification, bright-field image of the boxed area, showing that the apparent localization of *Fxna* mRNA to the oocyte is most likely due to an abundance of hybridization signal in granulosa cells of the cumulus oophorus. (**D**) Bright-field image of C. (**E**) High magnification, dark-field image of a 21-day-old ovary reiterating the presence of *Fxna* mRNA in granulosa cells of antral and preantral follicles, and the absence of hybridization (arrows) in oocytes. (**F**) Bright-field image of E. Scale bars: A, 100 μm; B,E,F, 20 μm; C,D, 400 μm; inset, 50 μm.

existence of a major mRNA species of 5.4 kb. The heavier, but minor, hybridizing species observed in ovary, kidney and adrenal gland may correspond to a transcript(s) resulting from the use of alternative transcription start sites or alternative polyadenylation signals. Because no hybridizing species smaller than 5.4 kb was detected, we conclude that the C5-530a2 mRNA is larger than the size predicted by computational analysis.

The C5-530a2 locus encodes a 5095 nt mRNA species whose expression increases at the time of ovarian follicle assembly

The region 5′ to the sequence reported for BC031519 contains an in-frame ATG site 1743 nt upstream from the predicted ATG. By comparing the sequence of PCR products derived from the amplification of reverse-transcribed ovarian RNA with the genomic sequence of contig AC096329, we determined that the C5-520a2 gene consists of 15 exons spread over 34,154 nt in chromosome 1 (see www.ensembl.org, June 2006). The mRNA coding region consists of 2697 nt, which would encode a predicted protein of 898 amino acids (Fig. 2).

RNA from ovaries at different developmental phases was analyzed by RNase-protection assay using two cRNA probes. Probe A (289 nt) corresponds to the C5-530a2 sequence obtained by gene differential display; probe B (406 nt) recognizes a sequence spanning the originally predicted ATG site in BC031519 (Fig. 3A). Consistent with the gene differential display results, C5-530a2 mRNA abundance detected with probe A increased significantly (P<0.02) at PN 48 hours, decreasing thereafter (P<0.02) to lower levels in adult ovaries (Fig. 3B). A similar profile was observed when probe B was hybridized to a pool of RNA samples from selected ages (Fig. 3C). Probe B recognized a single mRNA species, suggesting the absence of a C5-530a2 mRNA variant conforming to the mRNA predicted in BC031519. Based on these observations, we named the new gene (NM_184050) *Fxna* (for Felix-ina).

Fxna is a transmembrane peptidase of the M28 family localized to the endoplasmic reticulum

The predicted Fxna protein sequence is similar to members of peptidase family M28 (Rawlings and Barrett, 1995) (Fig. 4). Fig. 5 depicts the nucleotide sequence of Fxna and its predicted amino acid composition, showing the peptidase unit (underlined), the catalytic residues Asp201 and Glu245 (circled), and the metal ligand residues His199, Asp211, Glu246, Glu272 and His 348 (in squares).

Further analysis of the protein (http://www.cbs.dtu.dk/services/SignalP) predicted the absence of a canonical signal peptide. Thus, it is unlikely that Fxna is a secreted protein, a conclusion supported by a second analysis using a different software package (http://www.cbs.dtu.dk/services/SecretomeP). Instead, Fxna appears to be embedded into cellular membranes, via eight transmembrane domains located towards its C-terminus (Fig. 6A). The peptidase domain of Fxna is located toward the N-terminus (amino acid residues 163-393), a portion of the protein predicted to be localized on the external surface of cellular membranes (http://www.cbs.dtu.dk).

To identify the cellular membrane where Fxna is localized, we transfected COS-7 cells with Fxna-Flag and examined the cells by immunohistofluorescence-confocal microscopy using antibodies against the Flag epitope and against PDI, an

endoplasmic reticulum (ER)-specific marker. Fxna immunoreactivity colocalized with PDI (Fig. 6B-D), indicating that under basal conditions (i.e. in the absence of experimentally induced ligand-dependent activation of cell membrane receptors), Fxna is associated with ER membranes.

Fxna is selectively expressed in granulosa cells of the rat ovary

Ovaries collected 48 hours after birth were used to identify by in situ hybridization the cellular sites of *Fxna* mRNA expression in the rat ovary, using cRNA probe B labeled with ^{35}S-UTP. *Fxna* mRNA was abundantly expressed in newly formed ovarian follicles (Fig. 7A). Higher magnification revealed that *Fxna* mRNA was present in cells surrounding oocytes, i.e. granulosa cells (Fig. 7B), but not in oocytes (arrows). Examination of ovaries at PN-day 21 confirmed the selective localization of *Fxna* mRNA to ovarian follicles (Fig. 7C,D), and showed that atretic antral follicles do not contain *Fxna* mRNA (arrows). Within both preantral and antral follicles, *Fxna* mRNA was found only in granulosa cells (Fig. 7E,F), without detectable hybridization in oocytes (arrows).

Lentiviral-mediated delivery of siRNAs to the ovary decreases *Fxna* mRNA levels without triggering an interferon response

To determine the role of Fxna in the development of the ovary we employed an siRNA-mediated gene knock-down approach. Of five siRNAs tested, one (siRNA 436) silenced *Fxna* expression by more than 80% in the rat kidney cell line RK3E that expresses *Fxna* mRNA (Fig. 8A). None of the siRNAs tested showed off-target effects, as indicated by the unchanging levels of cyclophilin mRNA in the treated cells in comparison with untreated controls (Fig. 8A). After determining the biological potency and specificity of siRNA 436, the DNA sequence encoding siRNA 436 was cloned into pLV to generate viral particles producing shRNA.

Using this construct, a 'rescue' experiment was performed using an *Fxna* mRNA in which the region targeted by siRNA 436 carries silent nucleotide substitutions. 293T cells were transfected with expression vectors encoding the wild-type or the mutated *Fxna* mRNA form, plus the virus producing siRNA 436 (LV-sh436), and were cultured for 4 days. LV-sh436 suppressed wild-type *Fxna* mRNA expression, but failed to decrease mutant *Fxna* mRNA levels (Fig. 8B), demonstrating the specificity of the siRNA effect.

To evaluate the ability of LV-sh436 to decrease *Fxna* gene expression in the ovary, 1-day-old rat ovaries were placed in organ culture and treated for 4 days with LV-sh436 (4×10^6 TU per well, in 750 μl of medium). *Fxna* mRNA abundance was reduced by more than 90% in the LV-sh436-treated group as compared with LV-EGFP-treated controls (Fig. 9A). Ovaries treated with LV-siRNA 436 mism had *Fxna* mRNA levels indistinguishable from those seen in LV-EGFP-treated controls (LV-siRNA mism levels were 98.5% of those of the LV-EGFP group, data not shown). Despite this ineffectiveness we did not use this mutated siRNA further to avoid potential off-site effects resulting from the hypothetical ability of mismatched siRNAs to inhibit the translation of an unrelated gene(s) via a microRNA-like action (see the symposium on Understanding the RNAissance at www.nature.com/horizon).

A major difficulty encountered when using siRNAs (Sledz et al., 2003) and/or their delivery vectors (Bridge et al., 2003) is activation of the interferon system (Bridge et al., 2003; Sledz et al., 2003). To address this issue we adopted a recommended strategy (Bridge et al., 2003) and measured the mRNA encoded by the major interferon target gene 2′-5′ oligoadenylate synthase (*Oas1*) (Pebernard and Iggo, 2004; Samuel, 2001) in the same samples used to validate the effect of LV-sh436 on *Fxna* mRNA levels. *Oas1* mRNA levels were similar in ovaries treated with LV-EGFP, LV-sh436 and LV-sh436 mism (Fig. 9B), indicating the absence of an interferon response in the *Fxna*-knock-down ovaries.

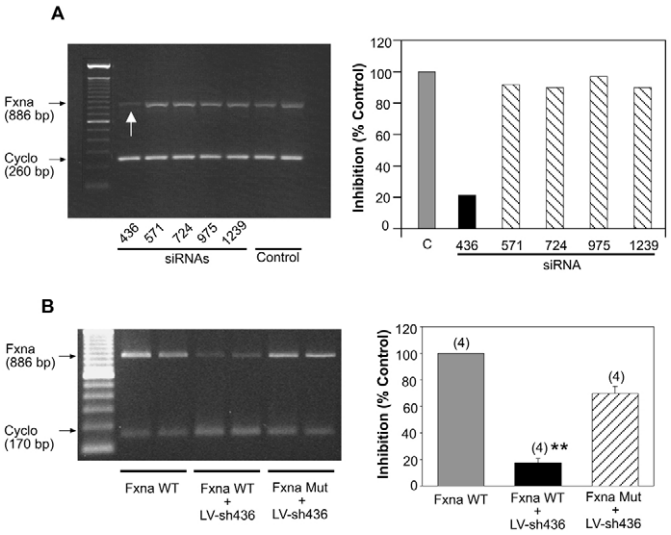

Fig. 8. Knock-down of *Fxna* expression using siRNAs and shRNAs. (**A**) Left panel shows that siRNAs decrease *Fxna* mRNA levels in RK3E cells 48 hours after transfection, as measured by semi-quantitative PCR. Each well was transfected with a different siRNA and the cellular RNA extracted 48 hours later. An 886 bp cDNA fragment was then PCR-amplified using primers annealing to sequences in the coding region of *Fxna* mRNA. Right panel is a quantitation of the changes detected in the gel shown in the left panel. (**B**) Left panel is a gel showing that mutating the third base of two codons in the sequence of *Fxna* mRNA targeted by LV-sh436 rescues *Fxna* mRNA from siRNA-induced silencing. The mutation creates a silent mutation as it does not change the encoded amino acids. 293T cells were transfected with a plasmid encoding wild-type *Fxna* mRNA or an *Fxna* mRNA carrying a silent mutation of the mRNA region targeted by LV-sh436. Six hours later the cells were infected with a lentiviral vector producing LV-sh436 or were left uninfected. The cells were then cultured for 4 days before extracting the RNA for semi-quantitative PCR. Right panel is a quantitation of the changes illustrated in the left panel. Fxna WT, wild-type *Fxna* mRNA; Fxna-Mut, Mutated *Fxna* mRNA. Bars are mean±s.e.m. and numbers in parentheses indicate the number of wells per group. **, $P<0.01$ versus both control groups.

Fxna deficiency disrupts follicular development and alters the structural organization of the ovary

To determine the cellular sites of LV expression, newborn rat ovaries were cultured for 4 days in the presence of LV-EGFP (4×10^6 TU per well in 750 μl of medium), before immunohistochemical detection of EGFP. As shown in Fig. 9C,D, infection was widespread, with EGFP-immunoreactive material observed in both somatic cells and oocytes. Infection of newborn ovaries with LV-sh436 for 4 days severely compromised the follicular structure as compared with that observed in control, LV-EGFP infected glands (Fig. 9E,F). The LV-

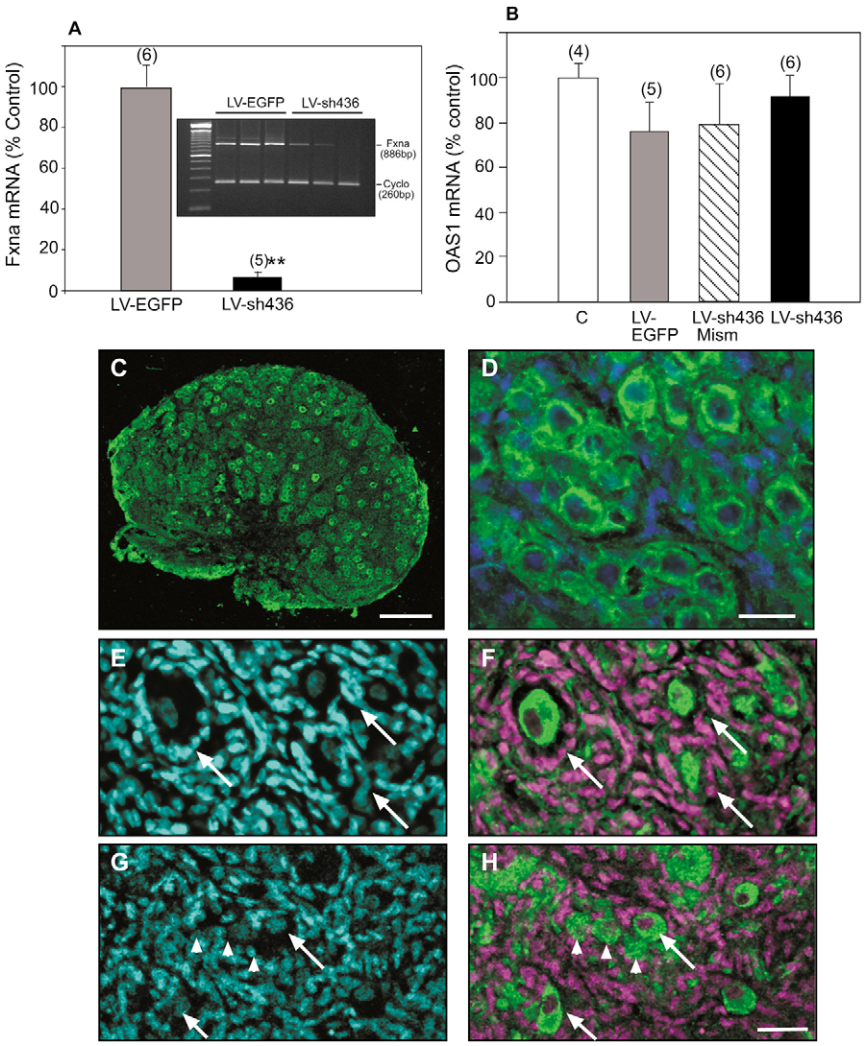

Fig. 9. Treatment of neonatal ovaries with LV-sh436 knocks down *Fxna* mRNA expression without generating an interferon-like response. Newborn rat ovaries were placed in organ culture and exposed for 4 days to LV-EGFP, LV-sh436 or LV-sh436 carrying several mismatches. The ovaries were then processed for either immunohistochemistry or RNA extraction. (**A**) LV-sh436 markedly reduced *Fxna* mRNA abundance. The bars are mean±s.e.m., and the numbers in parenthesis indicate the number of ovary pools per group (three ovaries per pool). **, $P<0.01$. The inset shows a representative gel. (**B**) Absence of an interferon response 4 days after infection of 1-day-old ovaries with LV-sh436 in organ culture, as determined by the normal content of *Oas1* mRNA measured in the treated ovaries. LV-EGFP, lentiviral vector alone; LV-sh436 Mism, LV carrying a sh436 sequence with nucleotide mismatches; LV-sh436, lentiviral vector carrying Fxna shRNA 436. (**C**,**D**) Lentiviral infection of neonatal rat ovaries in organ culture. The ovaries were explanted on the day of birth and exposed for 4 days to LV-EGFP. The glands were then fixed and subjected to immunohistofluorescence using polyclonal antibodies to EGFP. Cell nuclei were stained with Hoescht 33258 (blue). Low (C) and higher (D) magnification images depicting viral infection of both somatic cells and oocytes. (**E-H**) LV-sh436 infection of neonatal ovaries disrupts the structural organization of the ovary. The ovaries were treated as indicated above. Hoescht-stained cell nuclei are shown in light blue in E and G, and in magenta in F and H. Note the presence of primary follicles (arrows) in ovaries treated with LV-EGFP (E,F), and the aggregates of LV-sh436-expressing somatic cells (arrowheads) near isolated oocytes (arrows) in ovaries exposed to LV-sh436 (G,H). Scale bars: C, 200 μm; D, 10 μm; E-H, 25 μm.

sh436-infected ovaries exhibited aggregates of somatic cells excluding oocytes, and oocytes not encapsulated by granulosa cells (Fig. 9G,H).

To evaluate morphologically the consequences of Fxna deficiency on ovarian development, newborn rat ovaries were treated as above before conducting histopathologic and morphometric analyses of the glands. The ovaries treated with LV-EGFP showed an architecture typical of newborn ovaries grown in tissue culture (Kezele and Skinner, 2003), i.e. with many primordial follicles, but also showing an abundance of primary follicles (Fig. 10A,C). By contrast, the ovaries treated with LV-sh436 exhibited areas of striking immaturity (Fig. 10B) and overall structural disorganization characterized by solitary follicles containing up to four oocytes, nests of oocytes not associated with somatic cells, and aggregates of somatic cells not associated with oocytes (Fig. 10D). The number of 'naked' oocytes per ovary was similar in *Fxna*-knock-down ovaries and LV-EGFP-treated controls (Fig. 10E, left panel), but Fxna-deficient ovaries exhibited a marked ($P<0.01$) decrease in the total number of follicles per ovary (Fig. 10E, right panel). A more detailed analysis of the follicle populations affected revealed that all categories of follicles (primordial, primary and secondary) were significantly reduced in Fxna-deficient ovaries (Fig. 10F). These results indicate that the deficiency in follicular formation seen in the absence of Fxna is not secondary to a primary loss of oocytes.

The effects of Fxna deficiency on ovarian histogenesis are not related to alterations in either apoptotic or proliferative rates of ovarian cells

To determine if the alterations in ovarian histogenesis observed in Fxna-deficient ovaries were due to abnormal proliferation of somatic cells or somatic cell/oocyte death, we performed apoptosis and proliferation assays in LV-EGFP and LV-sh436-treated ovaries. No differences in the number of apoptotic cells per ovary as detected by TUNEL, or in the incorporation of BrdU into cell nuclei as detected by immunohistochemistry, were apparent between the two groups (data not shown).

DISCUSSION

The present study identifies a novel, hereto hypothetical gene as an important constituent of the regulatory machinery controlling definitive ovarian histogenesis. This gene, which we have termed *Fxna*, is selectively expressed in the granulosa cell compartment of ovarian follicles. *Fxna* mRNA is not only abundant in newly formed primordial follicles, but also in granulosa cells throughout the natural history of follicular growth, including the preovulatory antral stage. Noticeably, whereas the majority, if not all, preantral follicles express Fxna, a subpopulation of antral follicles with atretic features do not, suggesting that such follicles are in a

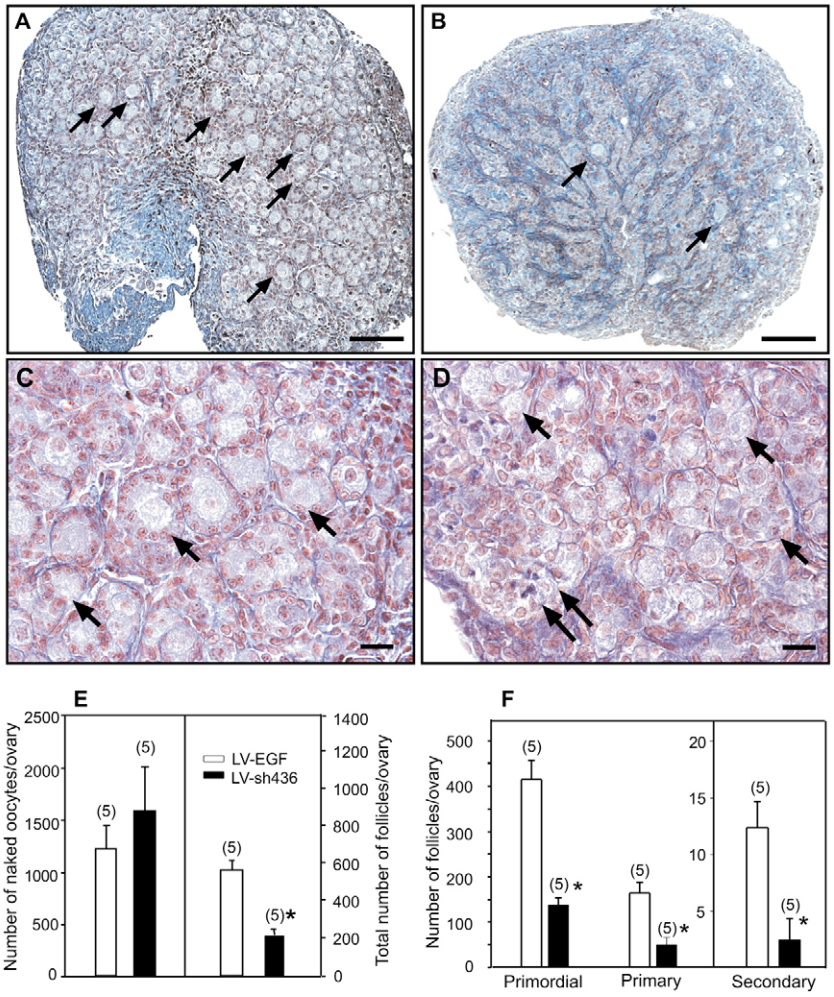

Fig. 10. Loss of Fxna disrupts ovarian histogenesis and reduces follicular formation. Neonatal rat ovaries were exposed for 4 days in organ culture to LV-EGFP or LV-sh436. One ovary from each animal was treated with LV-EGFP and the contralateral ovary was treated with LV-sh436. The glands were then fixed, serially sectioned and stained as described in Materials and methods. (**A**,**B**) Low magnification view of a control ovary (A) and of a *Fxna* knock-down gland (B) showing immature regions. Primary follicles with normal appearance (arrows) are fewer in number in LV-sh436-treated ovaries. Scale bars, 100 μm. (**C**,**D**) Higher magnification images illustrating the presence of multiple primary follicles (one layer of granulosa cells; arrows) in control (LV-EGFP-treated) ovaries (C), and the disorganization of somatic and germ cells in *Fxna* knock-down ovaries treated with LV-sh436 (D). Note the aggregates of somatic cells not associated with oocytes (pair of arrows) and the clusters of oocytes encapsulated by a rim of somatic cells (arrows). Scale bars, 20 μm. (**E**) The number of naked oocytes is similar in Fxna-deficient (black bars) and control (white bars) ovaries (left), but the total number of follicles per ovary is decreased in Fxna knock-down ovaries (right). (**F**) The number of follicles at all stages of development (primordial, primary and secondary) is reduced in Fxna-deficient ovaries (black bars). Bars are mean±s.e.m. Numbers in parentheses indicate the number of ovaries per group. *, $P<0.01$ versus LV-EGFP-treated group.

functional stage associated with loss of Fxna functions. The possibility that Fxna abundance is reduced in follicles undergoing atresia, a process initiated in earnest at the time of antral formation (Hsueh et al., 1994), deserves further consideration.

Analysis of its structural domains revealed that Fxna is a metallopeptidase that belongs to peptidase family M28 (Rawlings and Barrett, 1995). The structural characteristics of Fxna predict its existence as a membrane-bound protein, and our results demonstrate that in contrast to most peptidases expressed in reproductive organs (Fujiwara et al., 1999), Fxna is localized to the ER instead of the cell membrane. Previously described ER peptidases include endoplasmic reticulum aminopeptidase 1 (ERAP1) (Fruci et al., 2006), the related aminopeptidase leukocyte-derived arginine aminopeptidase (L-RAP, also called ERAP2) (Saveanu et al., 2005; Tanioka et al., 2003), and vitellogenic carboxypeptidase-like protein (Harris et al., 2006). The presence in Fxna of up to eight putative transmembrane domains resembles the hydropathy profile of site-2 protease (S2P), a zinc metallo-aminopeptidase required for the intramembranous proteolysis of sterol-regulatory-element-binding proteins (SREBPs) (Rawson et al., 1997). S2P is embedded in the ER via 5 transmembrane domains and releases the N-terminal domain of SREBPs within the ER membrane (Zelenski et al., 1999).

Peptidases bound to intracellular membranes may have fascinating functional properties as shown by the insulin-regulated aminopeptidase (IRAP), which is bound to intracellular membranes under basal conditions, but redistributes to the cell membrane in response to insulin stimulation (Keller, 2003). In type 2 diabetes, insulin action is impaired and the translocation of IRAP to the cell membrane fails to occur, suggesting that the absence of IRAP-mediated peptide processing on the cell membrane is an intrinsic component of this pathology. Although our results do not identify the mode of action of Fxna, they do demonstrate that Fxna is essential for the normalcy of definitive ovarian histogenesis. Silencing the *Fxna* gene strikingly disrupts ovarian structural organization. In Fxna-deficient ovaries, both the rate of follicle assembly and initiation of follicle growth are compromised, without detectable prior loss of oocytes. An even more remarkable feature is a widespread loss of somatic germ cell organization. Pregranulosa cells appear to encircle more than one oocyte, and many oocytes remain clustered in isolation without having been infiltrated by somatic cells, as would normally occur during follicular formation (Hirshfield, 1991).

Very few substrates for metallopeptidases have been identified. We do not know at present which proteins are hydrolyzed by Fxna. Because of its intracellular localization, Fxna might be necessary for the correct processing of proteins involved in cell signaling (Wolfe and Kopan, 2004) and/or transcriptional control (Rawson et al., 1997). Alternatively, it may act as a general degrading protease of transmembrane protein precursors. Nevertheless, the alterations in structural organization resulting from the loss of Fxna function in the ovary argue against the latter possibility, and suggest that systems affected by the deficiency may be those cell-to-cell communication

pathways required for definitive ovarian histogenesis. The two major morphogenic signaling complexes required for the organization of the very processes affected by Fxna deficiency are the Jagged-Notch (Artavanis-Tsakonas et al., 1999; Lai, 2004) and the Wnt-Frizzled (Cadigan and Nusse, 1997; Miller et al., 1999) signaling systems. Of note, both Notch2 and Frizzled1 receptors are expressed in granulosa cells throughout preantral development (Johnson et al., 2001; Richards et al., 2002), and in both cases loss of function results in abnormalities similar to those seen in Fxna-deficient ovaries (Hahn et al., 2005; Vainio et al., 1999). Should Fxna be involved in processing any of the basic and/or associated components of these systems, one would have to assume that it acts early in the processing pathway, as a proteolytic event that precedes the transport of such target proteins to the Golgi apparatus for covalent modifications and intracellular targeting.

In summary, our results identify a new regulatory system that operates in somatic granulosa cells to control ovarian development, and which appears to be required for proper structural organization of the ovary. The cellular systems targeted by the action of Fxna remain to be identified.

This work was supported by NIH grants HD-24870, RR-00163 and U54 HD18185. C.G.-R., V.T. and B.K. were supported in part by an NICHD TW/HD00668 Fogarty International Training grant. We thank Ricardo Ojeda for morphometric analysis; Maria E. Costa for performing the in situ hybridizations; and Dr Inder Verma (The Salk Institute, La Jolla, CA) for providing the lentivirus delivery system.

Supplementary material

Supplementary material for this article is available at http://dev.biologists.org/cgi/content/full/134/5/945/DC1

References

Altschul, S. F., Gish, W., Miller, W., Myers, E. W. and Lipman, D. J. (1990). Basic local alignment search tool. *J. Mol. Biol.* **215**, 403-410.

Artavanis-Tsakonas, S., Rand, M. D. and Lake, R. J. (1999). Notch signaling: cell fate control and signal integration in development. *Science* **284**, 770-776.

Benson, D. A., Karsch-Mizrachi, I., Lipman, D. J., Ostell, J. and Wheeler, D. L. (2006). GenBank. *Nucleic Acids Res.* **34**, D16-D20.

Bridge, A. J., Pebernard, S., Ducraux, A., Nicoulaz, A.-L. and Iggo, R. (2003). Induction of an interferon response by RNAi vectors in mammalian cells. *Nat. Genet.* **34**, 263-264.

Cadigan, K. M. and Nusse, R. (1997). Wnt signaling: a common theme in animal development. *Genes Dev.* **11**, 3286-3305.

Chomczynski, P. and Sacchi, N. (1987). Single-step method of RNA isolation by acid guanidinium thiocyanate-phenol-chloroform extraction. *Anal. Biochem.* **162**, 156-159.

Dees, W. L., Hiney, J. K., Schultea, T. D., Mayerhofer, A., Danilchik, M., Dissen, G. A. and Ojeda, S. R. (1995). The primate ovary contains a population of catecholaminergic neuron-like cells expressing nerve growth factor receptors. *Endocrinology* **136**, 5760-5768.

Dissen, G. A., Hill, D. F., Costa, M. E., Ma, Y. J. and Ojeda, S. R. (1991). Nerve growth factor receptors in the peripubertal rat ovary. *Mol. Endocrinol.* **5**, 1642-1650.

Dissen, G. A., Newman Hirshfield, A., Malamed, S. and Ojeda, S. R. (1995). Expression of neurotrophins and their receptors in the mammalian ovary is developmentally regulated: changes at the time of folliculogenesis. *Endocrinology* **136**, 4681-4692.

Dissen, G. A., Romero, C., Newman Hirshfield, A. and Ojeda, S. R. (2001). Nerve growth factor is required for early follicular development in the mammalian ovary. *Endocrinology* **142**, 2078-2086.

Dong, J., Albertini, D. F., Nishimori, K., Kumar, T. R., Lu, N. and Matzuk, M. M. (1996). Growth differentiation factor-9 is required during early ovarian folliculogenesis. *Nature* **383**, 531-535.

Dull, T., Zufferey, R., Kelly, M., Mandel, R. J., Nguyen, M., Trono, D. and Naldini, L. (1998). A third-generation lentivirus vector with a conditional packaging system. *J. Virol.* **72**, 8463-8371.

Follenzi, A., Ailles, L. E., Bakovic, S., Geuna, M. and Naldini, L. (2000). Gene transfer by lentiviral vectors is limited by nuclear translocation and rescued by HIV-1 pol sequences. *Nat. Genet.* **25**, 217-222.

Fruci, D., Ferracuti, S., Limongi, M. Z., Cunsolo, V., Giorda, E., Fraioli, R., Sibilio, L., Carroll, O., Hattori, A., van Endert, P. M. et al. (2006). Expression of endoplasmic reticulum aminopeptidases in EBV-B cell lines from healthy donors and in leukemia/lymphoma, carcinoma, and melanoma cell lines. *J. Immunol.* **176**, 4869-4879.

Fujiwara, H., Imai, K., Inoue, T., Maeda, M. and Fujii, S. (1999). Membrane-bound cell surface peptidases in reproductive organs. *Endocr. J.* **46**, 11-25.

Garcia-Rudaz, C., Luna, F., Dissen, G. A., Scior, T., Rawlings, N. D., Galimi, F. and Ojeda, S. R. (2004). Fxna, a novel gene differentially expressed in the rat ovary at the time of folliculogenesis is required for normal ovarian histogenesis. *Prog. 86th Ann. Mtg. Endocrine Soc.* p 89.

George, F. W. and Ojeda, S. R. (1987). Vasoactive intestinal peptide enhances aromatase activity in the neonatal rat ovary before development of primary follicles or responsiveness to follicle-stimulating hormone. *Proc. Natl. Acad. Sci. USA* **84**, 5803-5807.

Gilman, M. (1993). Ribonuclease protection assay. In *Current Protocols in Molecular Biology*. Vol. 1 (ed. F. M. Ausubel, R. Brent, R. E. Kingston, D. D. Moore, J. G. Seidman, J. A. Smith and K. Struhl), pp. 4.7.1-4.7.6. New York: Green Publishing and Wiley-Interscience.

Godin, I., Deed, R., Cooke, J., Zsebo, K., Dexter, M. and Wylie, C. C. (1991). Effects of the *steel* gene product on mouse primordial germ cells in culture. *Nature* **352**, 807-809.

Hahn, K. L., Johnson, J., Beres, B. J., Howard, S. and Wilson-Rawls, J. (2005). Lunatic fringe null female mice are infertile due to defects in meiotic maturation. *Development* **132**, 817-828.

Harris, J., Schwinn, N., Mahoney, J. A., Lin, H. H., Shaw, M., Howard, C. J., da Silva, R. P. and Gordon, S. (2006). A vitellogenic-like carboxypeptidase expressed by human macrophages is localized in endoplasmic reticulum and membrane ruffles. *Int. J. Exp. Pathol.* **87**, 29-39.

Hirshfield, A. N. (1991). Development of follicles in the mammalian ovary. *Int. Rev. Cytol.* **124**, 43-101.

Hirshfield, A. N. and DeSanti, A. M. (1995). Patterns of ovarian cell proliferation in rats during the embryonic period and the first three weeks postpartum. *Biol. Reprod.* **53**, 1208-1221.

Hsueh, A. J. W., Billig, H. and Tsafriri, A. (1994). Ovarian follicle atresia: a hormonally controlled apoptotic process. *Endocr. Rev.* **15**, 707-724.

Huang, E. J., Manova, K., Packer, A. I., Sanchez, S., Bachvarova, R. F. and Besmer, P. (1993). The murine steel panda mutation affects kit ligand expression and growth of early ovarian follicles. *Dev. Biol.* **157**, 100-109.

Johnson, J., Espinoza, T., McGaughey, R. W., Rawls, A. and Wilson-Rawls, J. (2001). Notch pathway genes are expressed in mammalian ovarian follicles. *Mech. Dev.* **109**, 355-361.

Keller, S. R. (2003). The insulin-regulated aminopeptidase: a companion and regulator of GLUT4. *Front. Biosci.* **8**, s410-s420.

Kezele, P. R. and Skinner, M. K. (2003). Regulation of ovarian primordial follicle assembly and development by estrogen and progesterone: endocrine model of follicle assembly. *Endocrinology* **144**, 3329-3337.

Lai, E. C. (2004). Notch signaling: control of cell communication and cell fate. *Development* **131**, 965-973.

Lara, H. E., Hill, D. F., Katz, K. H. and Ojeda, S. R. (1990). The gene encoding nerve growth factor is expressed in the immature rat ovary: effect of denervation and hormonal treatment. *Endocrinology* **126**, 357-363.

Lawson, K. A., Dunn, N. R., Roelen, B. A. J., Zeinstra, L. M., Davis, A. M., Wright, C. V. E., Korving, J. P. W. F. M. and Hogan, B. L. M. (1999). *Bmp4* is required for the generation of primordial germ cells in the mouse embryo. *Genes Dev.* **13**, 424-436.

Liang, L., Soyal, S. M. and Dean, J. (1997). FIGalpha, a germ cell specific transcription factor involved in the coordinate expression of the zona pellucida genes. *Development* **124**, 4939-4947.

Lipman, D. J. and Pearson, W. R. (1985). Rapid and sensitive protein similarity searches. *Science* **227**, 1435-1441.

Ma, Y. J., Dissen, G. A., Rage, F. and Ojeda, S. R. (1996). RNase protection assay. *Methods* **10**, 273-278.

Malamed, S., Gibney, J. A. and Ojeda, S. R. (1992). Ovarian innervation develops before initiation of folliculogenesis in the rat. *Cell Tissue Res.* **270**, 87-93.

Martin, K. J. and Pardee, A. B. (1999). Principles of differential display. *Methods Enzymol.* **303**, 234-257.

Miller, J. R., Hocking, A. M., Brown, J. D. and Moon, R. T. (1999). Mechanism and function of signal transduction by the Wnt/beta-catenin and Wnt/Ca2+ pathways. *Oncogene* **18**, 7860-7872.

Mungenast, A. and Ojeda, S. R. (2005). Expression of three gene families encoding cell-cell communication molecules in the prepubertal nonhuman primate hypothalamus. *J. Neuroendocrinol.* **17**, 208-219.

Nilsson, E., Parrott, J. A. and Skinner, M. K. (2001). Basic fibroblast growth factor induces primordial follicle development and initiates folliculogenesis. *Mol. Cell. Endocrinol.* **175**, 123-130.

Nilsson, E. E., Kezele, P. and Skinner, M. K. (2002). Leukemia inhibitory factor (LIF) promotes the primordial to primary follicle transition in rat ovaries. *Mol. Cell. Endocrinol.* **188**, 65-73.

Paredes, A., Romero, C., Dissen, G. A., DeChiara, T. M., Reichardt, L., Cornea, A., Ojeda, S. R. and Xu, B. (2004). TrkB receptors are required for follicular growth and oocyte survival in the mammalian ovary. *Dev. Biol.* **267**, 430-449.

Paredes, A., Garcia-Rudaz, C., Kerr, B., Tapia, V., Dissen, G. A., Costa, M. E., Cornea, A. and Ojeda, S. R. (2005). Loss of synaptonemal complex protein-1, a synaptonemal complex protein, contributes to the initiation of follicular assembly in the developing rat ovary. *Endocrinology* **146**, 5267-5277.
Parrott, J. A. and Skinner, M. K. (1999). Kit-ligand/stem cell factor induces primordial follicle development and initiates folliculogenesis. *Endocrinology* **140**, 4262-4271.
Pebernard, S. and Iggo, R. D. (2004). Determinants of interferon-stimulated gene induction by RNAi vectors. *Differentiation* **72**, 103-111.
Rajah, R. Glaser. E. M. and Hirshfield, A. N. (1992). The changing architecture of the neonatal ovary during histogenesis. *Dev. Dyn*. **194**, 177-192.
Rajkovic, A., Pangas, S. A., Ballow, D., Suzumori, N. and Matzuk, M. M. (2004). NOBOX deficiency disrupts early folliculogenesis and oocyte-specific gene expression. *Science* **305**, 1157-1159.
Rawlings, N. D. and Barrett, A. J. (1995). Evolutionary families of metallopeptidases. *Meth. Enzymol.* **248**, 183-228.
Rawlings, N. D., Morton, F. R. and Barrett, A. J. (2006). MEROPS: the peptidase database. *Nucleic Acids Res.* **34**, D270-D272.
Rawson, R. B., Zelenski, N. G., Nijhawan, D., Ye, J., Sakai, J., Hasan, M. T., Chang, T. Y., Brown, M. S. and Goldstein, J. L. (1997). Complementation cloning of S2P, a gene encoding a putative metalloprotease required for intramembrane cleavage of SREBPs. *Mol. Cell* **1**, 47-57.
Richards, J. S., Russell, D. L., Ochsner, S., Hsieh, M., Doyle, K. H., Falender, A. E., Lo, Y. K. and Sharma, S. C. (2002). Novel signaling pathways that control ovarian follicular development, ovulation, and luteinization. *Recent Prog. Horm. Res.* **57**, 195-220.
Samuel, C. E. (2001). Antiviral actions of interferons. *Clin. Microbiol. Rev.* **14**, 778-809.
Saveanu, L., Carroll, O., Lindo, V., Del Val, M., Lopez, D., Lepelletier, Y., Greer, F., Schomburg, L., Fruci, D., Niedermann, G. et al. (2005). Concerted peptide trimming by human ERAP1 and ERAP2 aminopeptidase complexes in the endoplasmic reticulum. *Nat. Immunol.* **6**, 689-697.
Simmons, D. M., Arriza, J. L. and Swanson, L. W. (1989). A complete protocol for *in situ* hybridization of messenger RNAs in brain and other tissues with radiolabeled single-stranded RNA probes. *J. Histotechnol.* **12**, 169-181.
Skinner, M. K. (2005). Regulation of primordial follicle assembly and development. *Hum. Reprod. Update* **11**, 461-471.
Sledz, C. A., Holko, M., deVeer, M. J., Silverman, R. H. and Williams, B. R. G. (2003). Activation of the interferon system by short-interfering RNAs. *Nat. Cell Biol.* **5**, 834-839.
Spears, N., Molinek, M. D., Robinson, L. L., Fulton, N., Cameron, H., Shimoda, K., Telfer, E. E., Anderson, R. A. and Price, D. J. (2003). The role of neurotrophin receptors in female germ-cell survival in mouse and human. *Development* **130**, 5481-5491.
Suzumori, N., Yan, C., Matzuk, M. M. and Rajkovic, A. (2002). Nobox is a homeobox-encoding gene preferentially expressed in primordial and growing oocytes. *Mech. Dev.* **111**, 137-141.
Tanioka, T., Hattori, A., Masuda, S., Nomura, Y., Nakayama, H., Mizutani, S. and Tsujimoto, M. (2003). Human leukocyte-derived arginine aminopeptidase. The third member of the oxytocinase subfamily of aminopeptidases. *J. Biol. Chem.* **278**, 32275-32283.
Tiscornia, G., Singer, O., Ilawa, M. and Verma, I. M. (2003). A general method for gene knockdown in mice by using lentiviral vectors expressing small interfering RNA. *Proc. Natl. Acad. Sci. USA* **100**, 1844-1848.
Trzeciak, W. H., Waterman, M. R., Simpson, E. R. and Ojeda, S. R. (1987). Vasoactive intestinal peptide regulates cholesterol side-chain cleavage cytochrome P-450 (P-450scc) gene expression in granulosa cells from immature rat ovaries. *Mol. Endocrinol.* **1**, 500-504.
Vainio, S., Heikkilä, M., Kispert, A., Chin, N. and McMahon, A. P. (1999). Female development in mammals is regulated by Wnt-4 signalling. *Nature* **397**, 405-409.
Wolfe, M. S. and Kopan, R. (2004). Intramembrane proteolysis: theme and variations. *Science* **305**, 1119-1123.
Zelenski, N. G., Rawson, R. B., Brown, M. S. and Goldstein, J. L. (1999). Membrane topology of S2P, a protein required for intramembranous cleavage of sterol regulatory element-binding proteins. *J. Biol. Chem.* **274**, 21973-21980.